

## Dynamics of the C-Terminal Region of TnI in the Troponin Complex in Solution

Tharin M. A. Blumenschein,\* Deborah B. Stone,<sup>†‡</sup> Robert J. Fletterick,<sup>†</sup> Robert A. Mendelson,<sup>‡</sup> and Brian D. Sykes\*

\*CIHR Group in Structure and Function and Department of Biochemistry, University of Alberta, Edmonton, Alberta T6G 2H7, Canada; and <sup>†</sup>Department of Biochemistry and Biophysics and <sup>‡</sup>Cardiovascular Research Institute, University of California, San Francisco, California 94143-2240

**ABSTRACT** The determination of crystal structures of the troponin complex (Takeda et al. 2003. *Nature*. 424:35–41; Vinogradova et al. 2005. *Proc. Natl. Acad. Sci. USA*. 102:5038–5043) has advanced knowledge of the regulation of muscle contraction at the molecular level. However, there are domains important for actin binding that are not visualized. We present evidence that the C-terminal region of troponin I (TnI residues 135–182) is flexible in solution and has no stable secondary structure. We use NMR spectroscopy to observe the backbone dynamics of skeletal [<sup>2</sup>H, <sup>13</sup>C, <sup>15</sup>N]-TnI in the troponin complex in the presence of Ca<sup>2+</sup> or EGTA/Mg<sup>2+</sup>. Residues in this region give stronger signals than the remainder of TnI, and chemical shift index values indicate little secondary structure, suggesting a very flexible region. This is confirmed by NMR relaxation measurements. Unlike TnC and other regions of TnI in the complex, the C-terminal region of TnI is not affected by Ca<sup>2+</sup> binding. Relaxation measurements and reduced spectral density analysis are consistent with the C-terminal region of TnI being a tethered domain connected to the rest of the troponin complex by a flexible linker, residues 137–146, followed by a collapsed region with at most nascent secondary structure.

### INTRODUCTION

In skeletal and cardiac muscle, contraction is regulated by changes in the Ca<sup>2+</sup> concentration inside the cell. These changes are sensed by the troponin (Tn)<sup>1</sup> complex and transmitted to the other components of the contractile unit. The troponin complex is formed by three subunits, troponin C (TnC), troponin I (TnI), and troponin T (TnT) (for reviews, see Sykes (1), Gordon et al. (2), Tobacman (3), and Farah and Reinach (4)). TnC is an EF-hand protein that can bind four Ca<sup>2+</sup> ions and is responsible for sensing the increase in calcium concentration. Two of its EF-hand sites, located in the C-domain, are high-affinity sites, capable of binding both Ca<sup>2+</sup> and Mg<sup>2+</sup>. These sites are occupied both during contraction and in the relaxed state. The other two EF-hand sites, located in the N-domain, are Ca<sup>2+</sup>-specific and have lower affinity, being occupied when the intracellular Ca<sup>2+</sup> levels rise during contraction, and empty in the relaxed state. This change in occupancy changes the interactions between TnC and TnI, and these conformational changes are transmitted to the rest of the thin filament, regulating muscle contraction.

TnI interacts with actin, TnC, and TnT. The interaction between TnI and actin inhibits muscle contraction and is independent of Ca<sup>2+</sup> in the absence of TnC (4). Two regions of TnI are capable of interacting with actin: the inhibitory region, comprising residues 104–115, and the C-terminal region, residues 148 and 182 (5). TnC and TnI interact in a

Ca<sup>2+</sup>-dependent manner. In the relaxed state, Ca<sup>2+</sup> concentrations inside the cell are low, and the only interaction between TnC and TnI is the structural interaction between the C-domain of TnC and the N-terminal region of TnI. When Ca<sup>2+</sup> levels inside the cell rise, the N-domain of TnC interacts with the “switch” region of TnI (residues 116–131 in skeletal TnI), removing the interactions between TnI and actin and, consequently, the inhibition. The interaction between TnI and TnT is a structural coiled-coil, involving residues 58–102 from TnI and 200–245 from TnT, in chicken fast skeletal muscle (6).

Besides TnI, TnT also interacts with tropomyosin and actin, keeping the troponin complex anchored to the thin filament in the absence of Ca<sup>2+</sup> and transmitting the conformational changes from the troponin complex to the rest of the regulatory unit (tropomyosin and seven monomers of actin).

We have previously reported dynamics measurements of TnC in the troponin complex (7). Here we study the dynamics of TnI in the troponin complex. The skeletal muscle isoform of TnI has 182 amino acids, but only the first 143 residues can be seen in the crystal structure of the troponin complex (6). The “missing” C-terminal region of TnI interacts with actin in muscle and is necessary to achieve wild-type levels of inhibition in the presence of TnC but absence of Ca<sup>2+</sup> (5). A nascent structure of this region has recently been determined (8).

A reconstituted troponin complex containing whole TnC, whole TnI, and the T2 domain of TnT was used to study the dynamics of TnI in the troponin complex. The T1 domain of TnT was not included because it causes aggregation of the

Submitted October 17, 2005, and accepted for publication December 27, 2005.

This article is dedicated to deceased colleague Robert A. Mendelson.

Address reprint requests to Brian D. Sykes, Tel: 780-492-5460; Fax: 780-492-0886; E-mail: Brian.Sykes@ualberta.ca.

© 2006 by the Biophysical Society

0006-3495/06/04/2436/09 \$2.00

doi: 10.1529/biophysj.105.076216

complex (9) and it does not interact with TnC and TnI (2). A group of peaks was much more intense than the others, making it difficult to analyze both groups of peaks at the same time. For that reason, we focused on the intense peaks, which were assigned to the key actin binding C-terminal region of TnI, comprising residues 136–182.

## MATERIALS AND METHODS

### Sample preparation

A uniformly deuterated deletion mutant of chicken skeletal muscle TnT (isoform TnT-3), corresponding to the T2 domain, was expressed and purified as described (9). Uniformly deuterated chicken skeletal TnC was prepared as described previously (10). Cysteine-free chicken skeletal muscle TnI was expressed from a plasmid kindly provided by Dr. Larry Smillie (11). [<sup>2</sup>H, <sup>13</sup>C, <sup>15</sup>N]-labeled cysteine-free TnI was expressed as previously described for TnC (12). Isolated inclusion bodies were resuspended in 8 M urea, 50 mM TrisCl pH 7.0, 1 mM EDTA. After clarification, the solution was loaded on a DEAE-Sephadex A-25 column equilibrated with the same buffer. The flow-through was collected, applied to a CM-Sephacose column equilibrated with the same buffer, and eluted with a 0–300 mM NaCl gradient. For further purification, the fractions containing TnI were dialyzed against the same buffer, with no salt and at pH 8.0, and applied to a CM-Sephacose column equilibrated with the same buffer at pH 8.0. Fractions containing TnI were dialyzed against 1% formic acid and lyophilized. The troponin complex containing these subunits was assembled and purified as described (9). The resulting complex was concentrated, dialyzed against 100 mM NH<sub>4</sub>HCO<sub>3</sub>, 0.1 mM dithiothreitol (DTT), and lyophilized.

For the Ca<sup>2+</sup> NMR sample, 12.2 mg of freeze-dried complex were dissolved in 200 μL of buffer containing 10 mM Hepes, 250 mM KCl, 5 mM CaCl<sub>2</sub>, 2 mM DTT, 0.03% sodium azide, and 0.2 mM 2,2-dimethyl-2-silapentane-5-sulfonic acid, in 90% H<sub>2</sub>O, 10% D<sub>2</sub>O. The pH was adjusted to 6.8. The solution was filtered using a microcentrifuge filter with 0.22 μm pore size, and transferred to an NMR tube (3 mm diameter). For the EGTA sample, 12.2 mg of freeze-dried complex were dissolved in 540 μL of buffer containing 10 mM Hepes, 250 mM KCl, 10 mM EGTA, 5 mM MgCl<sub>2</sub>, 2 mM DTT, 0.03% sodium azide, and 0.2 mM 2,2-dimethyl-2-silapentane-5-sulfonic acid, in 90% H<sub>2</sub>O, 10% D<sub>2</sub>O. The pH was adjusted to 7.1. The solution was filtered using a microcentrifuge filter with 0.22 μm pore size and transferred to an NMR tube (5 mm diameter). Expected free and bound concentrations of each ion and binding site were calculated with MaxChelator 2.50 (13), as described (7). This program can be obtained from <http://www.stanford.edu/~cpatton/maxc.html>. In the conditions used, <10% of the N-domain sites are expected to be occupied in the presence of EGTA/Mg<sup>2+</sup>.

### NMR spectroscopy

For chemical shift assignments of TnI in the troponin complex, [<sup>1</sup>H, <sup>15</sup>N]-TROSY-HSQC, three-dimensional (3D)-TROSY-HNCACB, and 3D-TROSY-HNCOCA spectra were acquired in a Varian INOVA 800 MHz spectrometer using BioPack (update version 2005-02-21, Varian, Palo Alto, CA) pulse sequences. For the backbone amide <sup>15</sup>N relaxation measurements, spectra were acquired on Varian INOVA 600 MHz and 800 MHz spectrometers. For relaxation time measurements, we used the T<sub>1</sub> or T<sub>2</sub> options in the gNhsqc BioPack (Varian) pulse sequence, based on pulse sequences developed by Kay and co-workers (14,15). These pulse sequences use <sup>1</sup>H 180° pulses during the relaxation period to eliminate the effects of cross correlation between dipolar and chemical shift anisotropy (CSA) relaxation mechanisms and were chosen to facilitate comparison with previously published data. For [<sup>1</sup>H]-<sup>15</sup>N nuclear Overhauser effect (NOE) heteronuclear relaxation measurements, the pulse sequence used was gNnoe (BioPack, Varian), based on a pulse sequence developed by Kay and co-

workers (15), with a delay inserted before each transient to allow for recovery of magnetization without unblinking of the amplifier. Relaxation delays were 10, 30, 50, 70, 90, 100, and 130 ms for T<sub>2</sub> and 0.01, 0.21, 0.41, 0.61, 0.81, 1.01, and 1.21 s for T<sub>1</sub>. The delay for nuclear Overhauser effect (NOE) build-up in the gNnoe experiments was 4 s, with a recovery delay of 6 s. In the no-nOe experiments, both delays were replaced by a recovery delay of 10 s. Two-dimensional (2D) NMR spectra were collected with 2048 (t<sub>2</sub>) × 96 (t<sub>1</sub>) complex points in TROSY mode and from 768 (t<sub>2</sub>) × 96 (t<sub>1</sub>) to 512 (t<sub>2</sub>) × 58 (t<sub>1</sub>) complex points when decoupling the indirectly detected dimension during acquisition. 3D NMR spectra were collected with 2048 (t<sub>3</sub>) × 82 (t<sub>1</sub>) × 32 (t<sub>2</sub>) (for HNCACB) or 2048 (t<sub>3</sub>) × 64 (t<sub>1</sub>) × 32 (t<sub>2</sub>) (for HNCOCA) complex points. All spectra were acquired at 30°C. All experimental free induced decays (FIDs) were processed with NMRPipe (16) and analyzed with NMRView (17). Linear prediction for up to half the number of experimental points was used in the indirectly detected dimension of experiments used for assigning. No linear prediction was used in the relaxation experiments. Data were zero-filled to the next power of 2 and multiplied by a sine-bell apodization function shifted by 90° before Fourier transformation. Data used for chemical shift assignments were also multiplied by a Gaussian function before Fourier transformation. Backbone amide <sup>15</sup>N T<sub>1</sub> and T<sub>2</sub> relaxation data were fitted to a two-parameter exponential decay using the “Rate Analysis” function of NMRView. (The error bars in the center and bottom panels of Fig. 3 represent the confidence intervals calculated by NMRView, using the noise level as an estimate for the standard deviation in intensity.) The intensity of the peaks in the nOe and no-nOe spectra was measured in NMRView, and the ratio between them was calculated using an in-house tk/tcl script. (The error bars in the top panel of Fig. 3 were calculated from the noise level in each spectrum.)

Reduced spectral density mapping analysis was performed according to the equations (18)

$$\sigma_{\text{NH}} = R_1(\text{NOE} - 1)\gamma_{\text{N}}/\gamma_{\text{H}}$$

$$J(0.87\omega_{\text{H}}) = 4\sigma_{\text{NH}}/(5d^2)$$

$$J(\omega_{\text{N}}) = [4R_1 - 5\sigma_{\text{NH}}]/[3d^2 + 4c^2]$$

$$J(0) = [6R_2 - 3R_1 - 2.72\sigma_{\text{NH}}]/[3d^2 + 4c^2],$$

where  $d = (\mu_0 h \gamma_{\text{N}} \gamma_{\text{H}} / 8\pi^2) (r^{-3})$  and  $c = \omega_{\text{N}} \Delta\sigma / \sqrt{3}$ .  $\gamma_{\text{N}}$  and  $\gamma_{\text{H}}$  are the gyromagnetic ratios of the <sup>1</sup>H and <sup>15</sup>N nuclei, respectively,  $\omega_{\text{H}}$  and  $\omega_{\text{N}}$  are the <sup>1</sup>H and <sup>15</sup>N Larmor frequencies,  $r$  is the internuclear <sup>1</sup>H-<sup>15</sup>N distance (1.02 Å), and  $\Delta\sigma$  is the CSA for <sup>15</sup>N (−160 ppm). The relaxation data acquired allowed us to evaluate the spectral density function in five different frequencies: J(0), J(61 MHz)—corresponding to J( $\omega_{\text{N}}$ ) in a 600 MHz spectrometer, J(81 MHz)—corresponding to J( $\omega_{\text{N}}$ ) in a 800 MHz spectrometer, J(522 MHz)—corresponding to J(0.87 $\omega_{\text{H}}$ ) in a 600 MHz spectrometer, and J(696 MHz)—corresponding to J(0.87 $\omega_{\text{H}}$ ) in a 800 MHz spectrometer. (The error bars in Fig. 4 were propagated from the errors for each of the relaxation measurements.)

## RESULTS

Skeletal troponin complex, reconstituted with <sup>2</sup>H-TnC, [<sup>2</sup>H, <sup>13</sup>C, <sup>15</sup>N]-TnI, and <sup>2</sup>H-TnT-T2, was used to acquire NMR spectra of TnI in the troponin complex in the presence of Ca<sup>2+</sup> and EGTA/Mg<sup>2+</sup> (Fig. 1). Peaks corresponding to the C-terminal region of TnI were much sharper and stronger than any other region of the protein, offering a unique opportunity to study the dynamics of that region. Peak widths are inversely proportional to the transverse relaxation time ( $\Delta\nu = 1/\pi T_2$ ), and sharper peaks indicate that this region is more flexible than the remainder of the protein. Since line widths cannot be accurately measured in 2D spectra, direct

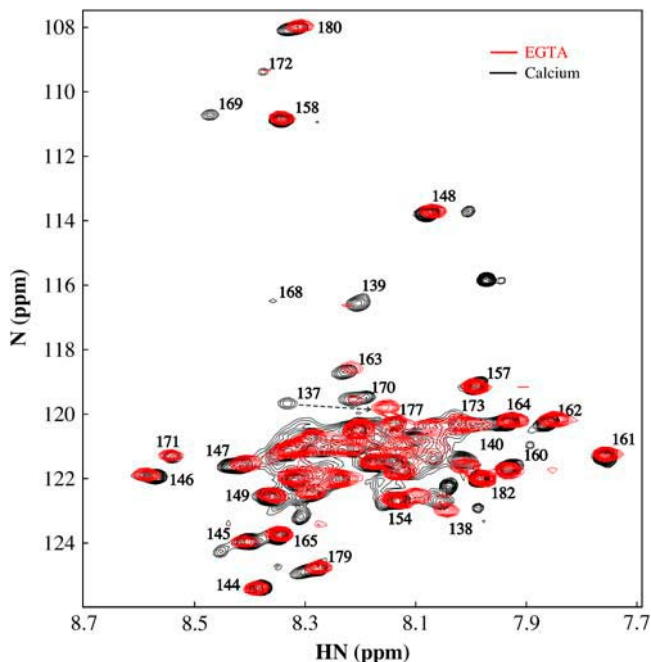


FIGURE 1 Comparison between 800 MHz  $\{^1\text{H}, ^{15}\text{N}\}$ -HSQC spectra of TnI in the troponin complex in the presence of  $\text{Ca}^{2+}$  (in black) and EGTA/ $\text{Mg}^{2+}$  (in red). Most of the visible peaks are not significantly affected by the presence or absence of  $\text{Ca}^{2+}$ . Some assignments are indicated in the figure. The residue most affected by the  $\text{Ca}^{2+}$  state is 137, which moves 0.2 ppm in the  $^1\text{H}$  dimension as indicated by the dashed line.

relaxation measurements are a more accurate way to study protein dynamics.

Fig. 1 shows 2D  $\{^1\text{H}, ^{15}\text{N}\}$ -HSQC NMR spectra of TnI in the troponin complex, with the vertical scale adjusted to

show only the intense peaks. The high intensity of the peaks corresponding to the C-terminal region of TnI, relative to the size of the troponin complex and the intensity of peaks from other regions of the protein, suggests that this is a very flexible region which moves independently from the rest of the complex. Most peaks are not affected by the presence or absence of  $\text{Ca}^{2+}$ , showing no change in chemical shift values between the two conditions used. The main exception to that is residue 137, which moves almost 0.2 ppm in the  $^1\text{H}$  dimension, as indicated by the dashed line in Fig. 1. Residue 136 could not be assigned in the presence of EGTA/ $\text{Mg}^{2+}$ .

Chemical shift assignments for N,  $\text{H}_\text{N}$ ,  $\text{C}_\alpha$ , and  $\text{C}_\beta$  atoms of residues 135–182 of TnI were obtained by sequential assignment, from 3D HNCACB and HNCOCA NMR experiments in the presence of  $\text{Ca}^{2+}$  and 3D HNCACB in the presence of EGTA/ $\text{Mg}^{2+}$ .

The chemical shift index (CSI) is a measurement of how much the chemical shift value for each atom differs from the standard value for that atom in a random coil environment and can therefore be used to determine the secondary structure of the protein (19). The  $^{13}\text{C}_\alpha$  CSI is not significantly affected by local sequence variation and is therefore more reliable than  $^1\text{H}_\text{N}$ ,  $^{13}\text{CO}$ , or  $^{15}\text{N}$  (20). CSI values were calculated by subtracting the reference value for random coil amino acids (21) from the assigned chemical shift for the residues in the C-terminal region of TnI in the presence of  $\text{Ca}^{2+}$  or EGTA/ $\text{Mg}^{2+}$ . To correct for deuterium isotope effects, 0.5 ppm were added to the result (22). The CSIs for the C-terminal region of TnI are presented in the top row of Fig. 2 in parts per million. The dashed lines represent the thresholds for any residue to be considered in an  $\alpha$ -helical (positive) or  $\beta$ -strand (negative) conformation. An  $\alpha$ -helical

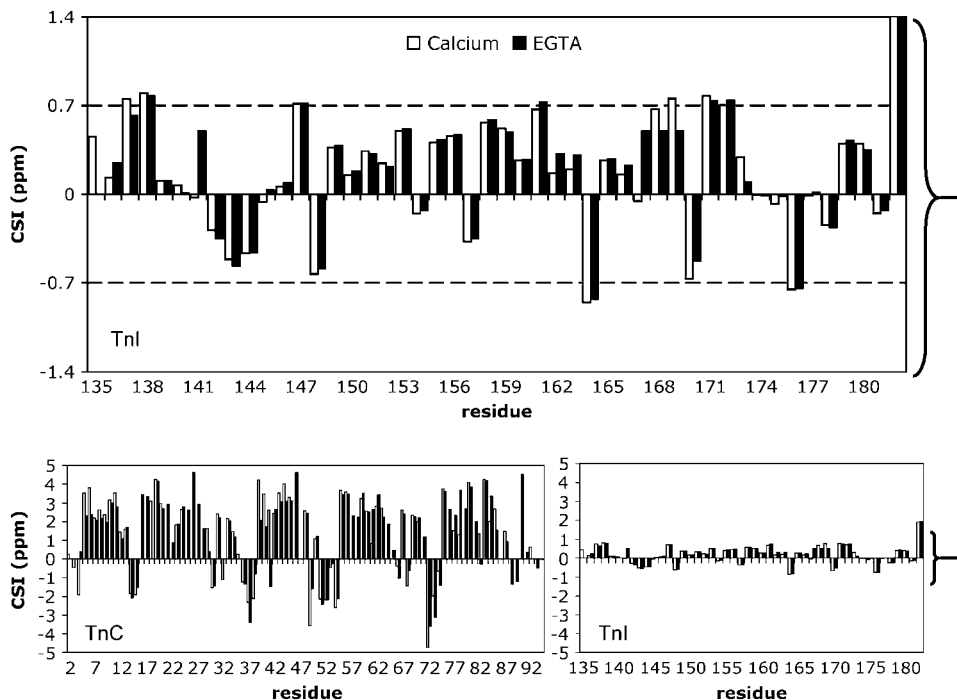


FIGURE 2  $^{13}\text{C}_\alpha$  CSI plots. (Top row) The visible region of TnI in the troponin complex, in the presence of  $\text{Ca}^{2+}$  or EGTA/ $\text{Mg}^{2+}$ . The dashed lines represent the threshold values for  $\alpha$ -helices (0.7 ppm) and  $\beta$ -strands (-0.7 ppm). (Bottom row) Comparison between TnI and the N-terminal domain of TnC in the troponin complex. Residues 135, 141, and 167–169 of TnI could not be assigned in the presence of EGTA/ $\text{Mg}^{2+}$ . Residues 1–3, 18, 47, and 86 of TnC could not be assigned in the presence of EGTA/ $\text{Mg}^{2+}$ , and residues 1, 16, 17, 25–28, 46, 47, 57, 58, 64, 65, 76, 79, 81, 86, 88–91, 93, and 94 of TnC could not be assigned in the presence of  $\text{Ca}^{2+}$ .

or  $\beta$ -strand segment is formed by a continuous stretch of at least three (for  $\beta$ -strands) or four (for  $\alpha$ -helices) residues in the protein (21). No stable secondary structure can be seen in this region of TnI.

A comparison between the CSIs for the N-terminal domain of TnC in the troponin complex and the C-terminal region of TnI, presented on the same scale, is shown in the bottom row of Fig. 2. TnC has well-defined secondary structure, which is reflected on chemical shift values of up to six times the threshold value and on average of three times the threshold value. The incipient quality of the secondary structure in the C-terminal region of TnI is reflected in the low indexes that most often do not achieve the threshold value for secondary structures.

Backbone amide  $^{15}\text{N}$  NMR relaxation measurements were performed for the C-terminal region of TnI in the troponin

complex and are presented in Fig. 3. The presence of  $\text{Ca}^{2+}$  or  $\text{EGTA}/\text{Mg}^{2+}$ , in general, did not affect the relaxation parameters.  $\{^1\text{H}\}\text{-}^{15}\text{N}$  heteronuclear NOE values were calculated from the ratio of the intensity of  $\{^1\text{H}\text{-}^{15}\text{N}\}$ -HSQC peaks in the presence and absence of proton saturation, as described in Materials and Methods, and presented in the top panel. The field at which the experiments were acquired strongly influences the NOE values due to effects on the CSA, and there was a significant difference between NOEs measured at 600 and 800 MHz, as expected. At 600 MHz, NOE ratios for many of the residues were too close to zero to be measured accurately. The measured values ranged from  $-0.53$  to  $0.28$  for most of this region of TnI, reaching  $-2.0$  for the most C-terminal residue. At 800 MHz, the NOE ratios could be measured for most residues and were between  $0.24$  and  $0.63$ . Residue 182 had the lowest NOE, at  $-1.1$ .

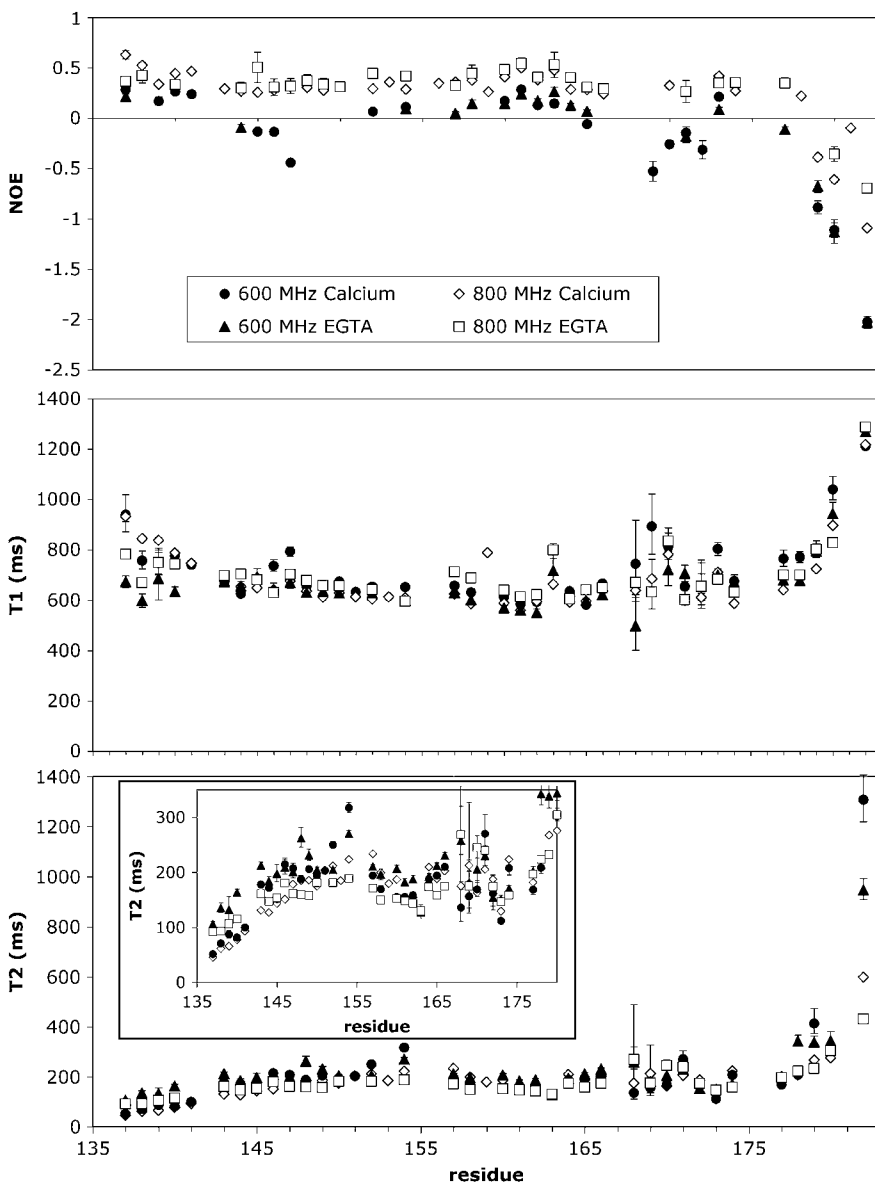


FIGURE 3 Backbone amide  $^{15}\text{N}$  NMR relaxation measurements for the visible region of TnI in the troponin complex, in the presence of  $\text{Ca}^{2+}$  and  $\text{EGTA}/\text{Mg}^{2+}$ , at two different fields: 600 MHz and 800 MHz. (●) In the presence of  $\text{Ca}^{2+}$  at 600 MHz; (▲) in the presence of  $\text{EGTA}/\text{Mg}^{2+}$  at 600 MHz; (◇) in the presence of  $\text{Ca}^{2+}$  at 800 MHz; and (□) in the presence of  $\text{EGTA}/\text{Mg}^{2+}$  at 800 MHz. (Top panel) NOE measurements; (center panel)  $T_1$  relaxation times; and (bottom panel)  $T_2$  relaxation times. The inset shows the lower region of the  $T_2$  relaxation times plot expanded.

Backbone amide  $^{15}\text{N}$   $T_1$  relaxation times are plotted in the central panel of Fig. 3. Residues 143–179 had relatively constant  $T_1$  times in both conditions and fields, with values between 500 and 800 ms. Only a few residues had  $T_1$  times above 800 ms. Between residues 137 and 141, inclusive, there was a larger variation of  $T_1$  times for each residue in the different conditions.  $T_1$  values were consistently higher in the presence of  $\text{Ca}^{2+}$  than in the presence of  $\text{EGTA}/\text{Mg}^{2+}$ . For residues 180 and 182 (residues 181, 155, and 142 are superimposed in the  $\{^1\text{H}, ^{15}\text{N}\}$ -HSQC spectrum and their relaxation parameters could not be measured),  $T_1$  times are longer, ranging from 828 ms to 1.29 s in both conditions.

Backbone amide  $^{15}\text{N}$   $T_2$  relaxation times were also measured and are plotted in the bottom panel of Fig. 3. The inset shows an expanded view of the lower region of the plot, with  $T_2$  times between 40 and 350 ms. All the residues, with exception of residue 182, fall within that region. It can be seen from the plot that the  $T_2$  relaxation times gradually increase for the first 10 residues, from residue 137 (the first residue for which  $T_2$  could be measured) to 146. For the first

five residues,  $T_2$  values are consistently larger in the presence of  $\text{EGTA}/\text{Mg}^{2+}$  than in the presence of  $\text{Ca}^{2+}$ . Between residues 147 and 177, the values of  $T_2$  remain relatively constant, between 100 and 300 ms. The five most C-terminal residues of the protein show another increase in  $T_2$  values, reaching up to 1.3 s for residue 182. For most of this region,  $T_2$  values are larger at 600 MHz than at 800 MHz, as expected from the effect of field intensity on transverse relaxation.

$^{15}\text{N}$  relaxation measurements were analyzed by reduced spectral density mapping (18,23). The intensity of the  $\{^1\text{H}, ^{15}\text{N}\}$ -HSQC peaks for the C-terminal region of TnI, together with the backbone amide  $^{15}\text{N}$  relaxation measurements for this region, indicate that this is a flexible region, which does not conform to the assumptions required for the commonly used model-free formalism (24,25).

The spectral density function was evaluated at five different frequencies, as described in Materials and Methods. The results are presented in Fig. 4. Fewer residues could be evaluated at the frequencies observed at 600 MHz, due to the

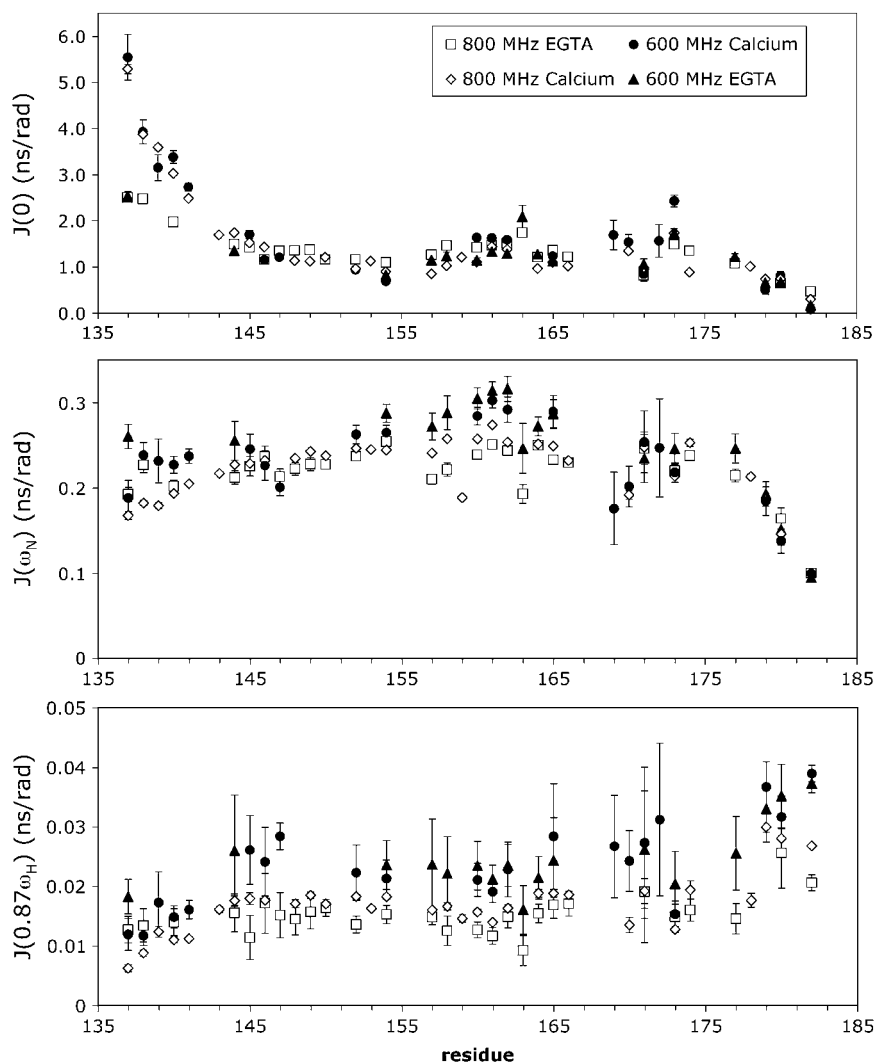


FIGURE 4 Spectral densities of backbone motions of the C-terminal region of TnI in the troponin complex, at five different frequencies, in nanoseconds/radians. (Top panel)  $J(0)$ ; (center panel)  $J(\omega_N)$ ; and (bottom panel)  $J(0.87\omega_H)$ . Spectral densities calculated from data acquired at 600 MHz are represented in black:  $J(0)$  in the top panel,  $J(61\text{ MHz})$  in the center panel, and  $J(522\text{ MHz})$  in the bottom panel. (●) In the presence of  $\text{Ca}^{2+}$ , and (▲) in the presence of  $\text{EGTA}/\text{Mg}^{2+}$ . Spectral densities calculated from data acquired at 800 MHz are represented in white:  $J(0)$  in the top panel,  $J(81\text{ MHz})$  in the center panel, and  $J(696\text{ MHz})$  in the bottom panel. (◇) In the presence of  $\text{Ca}^{2+}$ , and (□) in the presence of  $\text{EGTA}/\text{Mg}^{2+}$ .

lack of NOE data for these residues.  $J(0)$  shows clear difference between values in the presence of  $\text{Ca}^{2+}$  or EGTA/ $\text{Mg}^{2+}$  for the first five residues, whereas the remaining residues have very similar values for both fields and conditions. These initial residues have significantly higher values of  $J(0)$  in the presence of  $\text{Ca}^{2+}$  than in the presence of EGTA/ $\text{Mg}^{2+}$ , and the values decrease along the sequence. From residue 144 on,  $J(0)$  becomes constant until the last five residues when the value of  $J(0)$  drops again.

$J(\omega_N)$  shows field dependence for the first five residues and between residues 155–165. Its values are approximately constant along most of the C-terminal region of TnI, decreasing sharply along the last five residues.  $J(0.87\omega_H)$  increases gradually along the sequence of TnI, and  $J(522 \text{ MHz})$  is always larger than  $J(696 \text{ MHz})$ , as expected.

## DISCUSSION

Chemical shifts for the C-terminal region of TnI in the troponin complex were not significantly different in the presence of  $\text{Ca}^{2+}$  or EGTA/ $\text{Mg}^{2+}$ . This suggests that there are no conformational changes in this region in the presence or absence of  $\text{Ca}^{2+}$ , unlike TnC in the troponin complex (7). Although the interactions between TnC and TnI are known to depend on the presence of  $\text{Ca}^{2+}$  (2), our results confirm that those interactions do not affect the last 40 residues of TnI.

CSI analysis of this region of TnI shows that it has no stable secondary structure. NMR data reflect the behavior of a population of molecules, and the CSI reflects what fraction of the population has well-defined secondary structure. Using 2.8 ppm as the CSI for completely folded  $\alpha$  helices (26), the helical residues in the C-terminal region of TnI are, on average, 15% folded. Recently, a structure for this region was determined using NOE-based techniques (8). Whereas CSI is equally sensitive to folded and unfolded fractions of the population, NOE is more sensitive to the smaller distances between nuclei in the folded population. This can be seen from the following equations:

$$\begin{aligned}\delta_{\text{obs}} &= p_f \delta_f + p_u \delta_u \\ \text{NOE}_{\text{obs}} &= p_f \text{NOE}_f + p_u \text{NOE}_u \\ \text{NOE} &\propto 1/r_{ij}^6 \Rightarrow \\ \text{NOE}_{\text{obs}} &\propto p_f \left(1/r_{ij}^6\right)_f + p_u \left(1/r_{ij}^6\right)_u,\end{aligned}$$

where  $\delta_{\text{obs}}$  is the observed chemical shift,  $p_f$  is the folded fraction of the population,  $\delta_f$  is the chemical shift of the folded population,  $p_u$  is the unfolded fraction of the population,  $\delta_u$  is the chemical shift of the unfolded population,  $\text{NOE}_{\text{obs}}$  is the observed NOE,  $\text{NOE}_f$  and  $\text{NOE}_u$  are, respectively, the folded and unfolded NOE, and  $r_{ij}$  is the distance between the two nuclei for which the NOE is being measured. The observed chemical shift is the weighed

average of the chemical shifts in the population; the observed NOE is much more sensitive to nuclei that are close to each other, even if in a smaller fraction of the population. Since in unfolded states the nuclei tend to be farther apart, NOE-based structural determination can determine nascent structures that are only present in a small fraction of the population. The most helical residues in the C-terminal region of TnI are  $\sim 25\%$  folded and correspond to the ones that are above the threshold in Fig. 2.

Since random coil chemical shifts are associated with mobility (19), the CSI analysis indicates that the C-terminal of TnI is very flexible. This had already been demonstrated by the higher intensity for the peaks from this region when compared to the rest of the protein. Measurements of backbone amide  $^{15}\text{N}$  NMR relaxation parameters offer a more direct look at the dynamics of the C-terminal region of TnI. NOE ratios are relatively constant for most of the protein, with a pronounced decrease for the last four residues, indicating a very flexible C-terminal tail.

$T_1$  measurements show constant values for most of the residues measured, with slightly higher values for the first five residues, especially in the presence of calcium, and markedly higher values for the last four residues. Whereas the increase in  $T_1$  for the first five residues indicates less flexibility in that region due to the proximity of TnC, the longer  $T_1$  times at the C-terminus of TnI are a result of the higher flexibility of the C-terminal residues. The apparent correlation time for this region to TnI and the fields used place our  $T_1$  measurements around the minimum of the  $T_1 \times \tau_m$  plot (as represented in Spyropoulos et al. (27)), rendering  $T_1$  measurements especially insensitive to changes in mobility in the C-terminal region of TnI.

$T_2$  measurements, in contrast, start at relatively low values and increase gradually for the first 10 measured residues. This is followed by a region of constant  $T_2$ , ending with a sharp increase in  $T_2$  times for the last five residues of TnI. The C-terminal increase in  $T_2$  times is characteristic of flexible termini and widespread among proteins. The slow increase in  $T_2$  times between residues 137 and 146 is less common and indicates a gradual increase in mobility along the backbone of this region of TnI.  $T_2$  times for the C-terminal region of TnI suggest it is a tethered domain, analogous to a ball at the end of a chain. The domain is formed by a collapsed region of constant  $T_2$  times between residues 147 and 178, preceded by a ‘‘chain’’ of residues 137–146, which attach this region to the rest of the troponin complex.

A reduced spectral density mapping approach (18,23) was used to further analyze the relaxation data. The model-free approach (24,25) is the most commonly used method to analyze relaxation data. However, it assumes that the molecule is relatively rigid and its internal motions happen in a much faster timescale than the tumbling of the molecule ( $\tau_m \gg \tau_c$ ). Peak intensities, CSI, and the values of the relaxation parameters indicate that this is not the case for the C-terminal region of TnI.

$J(0.87\omega_H)$  values calculated from data acquired at 600 MHz were consistently higher than  $J(0.87\omega_H)$  values calculated from data acquired at 800 MHz. This shows that the spectral density function for the C-terminal region of TnI can be described by a sum of exponentials and can be accurately analyzed by the reduced spectral density mapping approach (23).

The  $J(0)$  term in the reduced spectral density mapping analysis contains contributions of the exchange term  $R_{ex}$ , which affects the transverse relaxation when present and for that reason is sometimes referred to as  $J_e(0)$  (18). The contribution of  $R_{ex}$  is highly dependent on magnetic field and can be explicitly calculated when relaxation data are acquired at more than one field (23). In the case of the C-terminal region of TnI, however, both transverse relaxation times  $T_2s$  and  $J(0)$  show almost identical values at the two different fields, indicating that any contribution of an exchange term would be minimal and does not need to be calculated explicitly.

High  $J(0)$  values are indicative of slow motions (millisecond-microsecond), whereas  $J(0.87\omega_H)$  is sensitive only to fast internal motions in the picosecond-nanosecond timescale (28). Taken together, the spectral density plots (Fig. 4) indicate that the first five measured residues are dominated by slow motions, which are more prominent in the presence of  $Ca^{2+}$  than in the presence of EGTA/ $Mg^{2+}$ , suggesting a different anchoring for the tethered domain in the presence of  $Ca^{2+}$  or EGTA/ $Mg^{2+}$ . A central region containing ~30 residues (roughly residues 145–175) has a smaller amount of slow motions, with the  $J(0)$  constant around 1; and the C-terminal tail is very flexible, dominated by fast motions. Underlying that pattern, fast motions increase constantly from residue 137 to 182.

An apparent correlation time can be calculated for the central region encompassing residues 145–175, from the spectral density functions (18), according to the formula

$$\tau_m = \omega_N^{-1} \left( \frac{J(0) - J(\omega_N)}{J(\omega_N)} \right)^{1/2}$$

The resulting value is ~4 ns, which corresponds roughly to a molecular mass of 8 kDa (27). This is the same apparent molecular weight found from a simple relationship between transverse relaxation rate and molecular weight, derived from a number of proteins (7,29), and corresponds to ~70 residues. This is more than the 47 residues contained in the C-terminal region of TnI and likely reflects the fact that this region is attached to the much larger troponin complex and is not rotating freely in solution. It also indicates that the C-terminal region of TnI is collapsed in the context of the troponin complex, as suggested by the NOE,  $T_2$ , and  $J(0)$  plots. At the same time, NOE values indicate that this is not a rigid 8-kDa domain. Expected NOE values for a rigid domain that size are ~0.8.

Although the dynamics data show that the C-terminal of TnI is collapsed, the CSI shows no sign of stable secondary structure. Although this may seem contradictory at first,

different models in polymer theory predict at least some degree of collapse for an unstructured protein independently of secondary structure (30). NMR spectroscopy describes the average ensemble of molecules in the sample; and therefore the possibility of transient secondary structure being formed in part of the ensemble, at levels too low to affect the average, cannot be excluded.

The picture that emerges for the C-terminal region, encompassing residues 137–182 of TnI, is that of a tethered collapsed domain, very flexible and with at most nascent secondary structure. This kind of domain had already been suggested by King et al. (9) as consistent with small angle neutron scattering data.

The domain is attached to the rest of the troponin complex only by the interaction between TnC and the “switch” region of TnI, which is known to be a  $Ca^{2+}$ -dependent interaction (31). Nonetheless, the switch region does not become completely flexible in the presence of EGTA/ $Mg^{2+}$ , since it cannot be visualized as sharper NMR peaks as observed for the C-terminal region. Rather, it stays close to TnC, as suggested by the crystal structure (6). The initial residues of the C-terminal region (137–141) become significantly more flexible in the presence of EGTA/ $Mg^{2+}$ , indicating a change in the interactions between TnC and the preceding regions of TnI.

Despite being collapsed, fast motions (in the picosecond-nanosecond timescale) in the C-terminal region of TnI increase proportionally to the distance from the attachment point to the rest of the troponin complex. This suggests that along the whole sequence of this region, the point of attachment is a main factor limiting fast motions.

In the muscle, the C-terminal region of TnI interacts with actin in the relaxed state and is necessary for the inhibition of muscle contraction in the presence of TnC and absence of  $Ca^{2+}$  (5). This suggests that although this region of TnI is mostly unstructured in the presence of  $Ca^{2+}$ , it becomes structured upon interaction with actin, as many examples of unstructured proteins and domains that fold upon binding to their targets (32). The coupling of folding and binding can offer high specificity at a modest affinity, since there is a balance between the enthalpic energy in the bound state and the entropic energy in the free, unfolded state. This is especially important for complexes that need to dissociate easily. To respond to the  $Ca^{2+}$  signal and start muscle contraction, TnI and actin have to be able to dissociate promptly.

Once dissociated from actin in the presence of  $Ca^{2+}$ , the region of the troponin complex that contains the C-terminal region of TnI is at a larger distance from actin than in the absence of  $Ca^{2+}$ , when TnI is interacting with actin. The “fly-casting mechanism” proposed for unstructured proteins (33) would allow TnI to bind to actin from that larger distance, folding and “reeling in” the whole troponin complex to the position that it occupies once TnI is bound to actin. According to this model, the C-terminal region of TnI remains unfolded when not interacting with actin and has a

larger radius of gyration than it would when folded. When TnI approaches actin, weak interactions between unfolded TnI and actin can therefore begin to occur at a much larger distance than if TnI had to be folded. As these weak interactions occur, they increase the likelihood of other residues in TnI also interacting with actin, the enthalpic energy of the interactions compensates for the increased entropy of the unfolded state, and the C-terminal region of TnI assumes its folded conformation. The interaction between this region of TnI and actin, which holds the troponin complex in place in the absence of  $\text{Ca}^{2+}$ , is likely part of the extra mass located in the absence of  $\text{Ca}^{2+}$  on the outer domain of actin by electron microscopy (8,34,35).

The homologous C-terminal region in cardiac TnI contains a few mutations associated with familial hypertrophic cardiomyopathy, K205S, G202S, and  $\Delta\text{K}182$ . However, there is very limited functional information available about mutations in that region (36). The C-terminal region is very similar in the skeletal and cardiac isoforms of TnI, with >75% identity. It is therefore expected that both have the same structural properties, and the C-terminal region of cardiac TnI should also be unstructured when not bound to actin. Degradation of this region is associated with ischemia and myocardial stunning (36). Being unstructured when not bound to actin, this region of TnI can be particularly susceptible to proteolysis.

Although the crystal structures of the troponin complex did not show the C-terminal region of TnI, NMR dynamics reveals that it is intrinsically unstructured when not bound to actin. The coupling between folding and binding to actin allows the C-terminal of TnI to bind actin effectively from the  $\text{Ca}^{2+}$  state and to dissociate easily to allow muscle contraction.

We thank Dr. Larry Smillie for the kind gift of the pET3a plasmid for optimized expression of cysteineless chicken skeletal TnI; David Corson and Galina Malanina for expression, purification, and assembly of the troponin complex; and Dr. Pascal Mercier for the assistance in calculating expected values for the relaxation parameters. We thank the Canadian National High Field NMR Centre (NANUC) for its assistance and use of facilities.

Operation of NANUC is funded by the Canadian Institutes of Health Research, the Natural Science and Engineering Research Council of Canada, and the University of Alberta. This work was supported by grants from the Canadian Institutes of Health Research and the National Institutes of Health (grant AR45659). T.M.A.B. was the recipient of an Alberta Heritage Foundation for Medical Research Postdoctoral Fellowship.

## REFERENCES

1. Sykes, B. D. 2003. Pulling the calcium trigger. *Nat. Struct. Biol.* 10: 588–589.
2. Gordon, A. M., E. Homsher, and M. Regnier. 2000. Regulation of contraction in striated muscle. *Physiol. Rev.* 80:853–924.
3. Tobacman, L. S. 1996. Thin filament-mediated regulation of cardiac contraction. *Annu. Rev. Physiol.* 58:447–481.
4. Farah, C. S., and F. C. Reinach. 1995. The troponin complex and regulation of muscle contraction. *FASEB J.* 9:755–767.
5. Ramos, C. H. 1999. Mapping subdomains in the C-terminal region of troponin I involved in its binding to troponin C and to thin filament. *J. Biol. Chem.* 274:18189–18195.
6. Vinogradova, M. V., D. B. Stone, G. G. Malanina, C. Karatzaferi, R. Cooke, R. A. Mendelson, and R. J. Fletterick. 2005.  $\text{Ca}^{2+}$ -regulated structural changes in troponin. *Proc. Natl. Acad. Sci. USA.* 102:5038–5043.
7. Blumenschein, T. M., D. B. Stone, R. J. Fletterick, R. A. Mendelson, and B. D. Sykes. 2005. Calcium-dependent changes in the flexibility of the regulatory domain of TnC in the troponin complex. *J. Biol. Chem.* 280:21924–21932.
8. Murakami, K., F. Yumoto, S. Ohki, T. Yasunaga, M. Tanokura, and T. Wakabayashi. 2005. Structural basis for  $\text{Ca}^{2+}$ -regulated muscle relaxation at interaction sites of troponin with actin and tropomyosin. *J. Mol. Biol.* 352:178–201.
9. King, W. A., D. B. Stone, P. A. Timmins, T. Narayanan, A. A. M. von Brasch, R. A. Mendelson, and P. M. G. Curmi. 2005. Solution structure of the chicken skeletal muscle troponin complex via small-angle neutron and x-ray scattering. *J. Mol. Biol.* 345:797–815.
10. Stone, D. B., P. A. Timmins, D. K. Schneider, I. Krylova, C. H. I. Ramos, F. C. Reinach, and R. A. Mendelson. 1998. The effect of regulatory  $\text{Ca}^{2+}$  on the in situ structures of troponin C and troponin I: a neutron scattering study. *J. Mol. Biol.* 281:689–704.
11. Dargis, R., J. R. Pearlstone, I. Barrette-Ng, H. Edwards, and L. B. Smillie. 2002. Single mutation (A162H) in human cardiac troponin I corrects acid pH sensitivity of  $\text{Ca}^{2+}$ -regulated actomyosin S1 ATPase. *J. Biol. Chem.* 277:34662–34665.
12. Slupsky, C. M., C. M. Kay, F. C. Reinach, L. B. Smillie, and B. D. Sykes. 1995. Calcium-induced dimerization of troponin C: mode of interaction and use of trifluoroethanol as a denaturant of quaternary structure. *Biochemistry.* 34:7365–7375.
13. Patton, C., S. Thompson, and D. Epel. 2004. Some precautions in using chelators to buffer metals in biological solutions. *Cell Calcium.* 35: 427–431.
14. Kay, L. E., L. K. Nicholson, F. Delaglio, A. Bax, and D. A. Torchia. 1992. Pulse sequences for removal of the effects of cross correlation between dipolar and chemical-shift anisotropy relaxation mechanisms on the measurement of heteronuclear  $T_1$  and  $T_2$  values in proteins. *J. Magn. Reson.* 97:359–375.
15. Farrow, N. A., R. Muhandiram, A. U. Singer, S. M. Pascal, C. M. Kay, G. Gish, S. E. Shoelson, T. Pawson, J. D. Forman-Kay, and L. E. Kay. 1994. Backbone dynamics of a free and phosphopeptide-complexed Src homology 2 domain studied by  $^{15}\text{N}$  NMR relaxation. *Biochemistry.* 33:5984–6003.
16. Delaglio, F., S. Grzesiek, G. W. Vuister, G. Zhu, J. Pfeifer, and A. Bax. 1995. NMRPipe: a multidimensional spectral processing system based on UNIX pipes. *J. Biomol. NMR.* 6:277–293.
17. Johnson, B. A., and R. A. Blevins. 1994. NMR View—a computer-program for the visualization and analysis of NMR data. *J. Biomol. NMR.* 4:603–614.
18. Bracken, C., P. A. Carr, J. Cavanagh, and A. G. Palmer 3rd. 1999. Temperature dependence of intramolecular dynamics of the basic leucine zipper of GCN4: implications for the entropy of association with DNA. *J. Mol. Biol.* 285:2133–2146.
19. Wishart, D. S., and B. D. Sykes. 1994. Chemical shifts as a tool for structure determination. *Methods Enzymol.* 239:363–392.
20. Schwartzinger, S., G. J. A. Kroon, T. R. Foss, J. Chung, P. E. Wright, and H. J. Dyson. 2001. Sequence-dependent correction of random coil NMR chemical shifts. *J. Am. Chem. Soc.* 123:2970–2978.
21. Wishart, D. S., and B. D. Sykes. 1994. The  $^{13}\text{C}$  chemical-shift index: a simple method for the identification of protein secondary structure using  $^{13}\text{C}$  chemical-shift data. *J. Biomol. NMR.* 4:171–180.
22. Gardner, K. H., and L. E. Kay. 1998. The use of  $^2\text{H}$ ,  $^{13}\text{C}$ ,  $^{15}\text{N}$  multi-dimensional NMR to study the structure and dynamics of proteins. *Annu. Rev. Biophys. Biomol. Struct.* 27:357–406.
23. Farrow, N. A., O. Zhang, A. Szabo, D. A. Torchia, and L. E. Kay. 1995. Spectral density function mapping using  $^{15}\text{N}$  relaxation data exclusively. *J. Biomol. NMR.* 6:153–162.

24. Lipari, G., and A. Szabo. 1982. Model-free approach to the interpretation of nuclear magnetic resonance relaxation in macromolecules. *J. Am. Chem. Soc.* 104:4546–4559.
25. Mandel, A. M., M. Akke, and A. G. Palmer 3rd. 1995. Backbone dynamics of Escherichia coli ribonuclease HI: correlations with structure and function in an active enzyme. *J. Mol. Biol.* 246: 144–163.
26. Yao, J., J. Chung, D. Eliezer, P. E. Wright, and H. J. Dyson. 2001. NMR structural and dynamic characterization of the acid-unfolded state of apomyoglobin provides insights into the early events in protein folding. *Biochemistry.* 40:3561–3571.
27. Spyropoulos, L., S. M. Gagné, W. Gronwald, L. E. Kay, and B. D. Sykes. 1998. NMR studies of protein side-chain dynamics: examples of anti-freeze and calcium regulatory proteins. In *Protein Dynamics, Function, and Design*. O. Jardetzky and J. F. Lefevre, editors. Plenum Press, New York. 147–162.
28. Dyson, H. J., and P. E. Wright. 2001. Nuclear magnetic resonance methods for elucidation of structure and dynamics in disordered states. *Methods Enzymol.* 339:258–270.
29. Lindhout, D. A. 2005. An NMR investigation of Troponin I within the cardiac troponin complex and the effects on calcium induced cardiac muscle contraction: The 'I' in team. Ph.D. thesis, University of Alberta, Edmonton, Canada.
30. Bright, J. N., T. B. Woolf, and J. H. Hoh. 2001. Predicting properties of intrinsically unstructured proteins. *Prog. Biophys. Mol. Biol.* 76:131–173.
31. Tripet, B., J. E. Van Eyk, and R. S. Hodges. 1997. Mapping of a second actin-tropomyosin and a second troponin C binding site within the C terminus of troponin I, and their importance in the  $Ca^{2+}$ -dependent regulation of muscle contraction. *J. Mol. Biol.* 271:728–750.
32. Dyson, H. J., and P. E. Wright. 2002. Coupling of folding and binding for unstructured proteins. *Curr. Opin. Struct. Biol.* 12:54–60.
33. Shoemaker, B. A., J. J. Portman, and P. G. Wolynes. 2000. Speeding molecular recognition by using the folding funnel: the fly-casting mechanism. *Proc. Natl. Acad. Sci. USA.* 97:8868–8873.
34. Lehman, W., M. Rosol, L. S. Tobacman, and R. Craig. 2001. Troponin organization on relaxed and activated thin filaments revealed by electron microscopy and three-dimensional reconstitution. *J. Mol. Biol.* 307:739–744.
35. Pirani, A., C. Xu, V. Hatch, R. Craig, L. S. Tobacman, and W. Lehman. 2005. Single particle analysis of relaxed and activated muscle thin filaments. *J. Mol. Biol.* 346:761–772.
36. Li, M. X., X. Wang, and B. D. Sykes. 2004. Structural based insights into the role of troponin in cardiac muscle pathophysiology. *J. Muscle Res. Cell Motil.* 25:559–579.